

D₂ Receptors Regulate Dopamine Transporter Function via an ERK 1/2-Dependent and PI3 Kinase-Independent Mechanism

Elizabeth A. Bolan, Bronwyn Kivell, Vanaja Jalgam, Murat Oz, Lankupalle D. Jayanthi, Yang Han,
Namita Sen, Eneki Urizar, Ivone Gomes, Lakshmi A. Devi, Sammanda Ramamoorthy Jonathan
Javitch^{*}, Agustin Zapata^{*}, and Toni S. Shippenberg^{*}

*Integrative Neuroscience Section, NIDA IRP/NIH/DHHS, 333 Cassell Drive, Baltimore, MD
21224.: E.A.B, B.K, V.J., M.O., A.Z., T.S.S.*

*Department of Neurosciences, Division of Neuroscience Research, Medical University of South
Carolina, 173 Ashley Avenue, Charleston, SC 29425: L.D.J., S.R.*

*Center for Molecular Recognition and Departments of Psychiatry and Pharmacology, College of
Physicians and Surgeons, Columbia University, 630 W. 168th Street, New York, NY 10032:
Y.H., N.S., E.U., J.J.*

*Department of Pharmacology and Biological Chemistry, Mount Sinai School of Medicine, New
York, NY 10029: I.G., L.A.D.*

^{*} These authors contributed equally to the work

Running Title: D2R regulation of dopamine transporter function

Correspondences to:

Toni S. Shippenberg

Integrative Neuroscience Section, NIDA IRP/NIH/DHHS

333 Cassell Dr, Baltimore, MD 21224

Tel: 410 550 1451 ext 14

Fax: 410 550 1692

Email: tshippen@intra.nida.nih.gov

Number of text pages: 29

Number of tables: 0

Number of figures: 9

Number of references: 44

Number of words in Abstract: 250

Number of words in Introduction: 719

Number of words in Discussion: 1520

Abbreviations: DAT, dopamine transporter; D_{2S}R, D₂ receptor short splice variant; WT, wild type; BRET, bioluminescence resonance energy transfer

ABSTRACT

The dopamine transporter (DAT) terminates dopamine (DA) neurotransmission by reuptake of DA into presynaptic neurons. Regulation of DA uptake by D₂ dopamine receptors (D₂R) has been reported. The high affinity of DA and other DAT substrates for the D₂R, however, has complicated investigation of the intracellular mechanisms mediating this effect. The present studies used the fluorescent DAT substrate, 4-[4-(diethylamino)-styryl]-N-methylpyridinium iodide (ASP⁺) with live cell imaging techniques to identify the role of two D₂R-linked signaling pathways, extracellular signal-regulated kinases 1 and 2 (ERK 1/2) and phosphoinositide 3 kinase (PI3K), in mediating D₂R regulation of DAT. Addition of the D₂/D₃ receptor agonist quinpirole (0.1-10 μ M) to human embryonic kidney cells co-expressing human DAT and D₂ receptor (short splice variant, D_{2S}R) induced a rapid, concentration-dependent and pertussis toxin-sensitive increase in ASP⁺ accumulation. The D₂/D₃ agonist, PD128907 also increased ASP⁺ accumulation. D_{2S}R activation increased phosphorylation of ERK 1/2 and Akt, a major target of PI3K. The MEK inhibitor, PD98059, prevented the quinpirole-evoked increase in ASP⁺ accumulation, whereas inhibition of PI3K was without effect. Fluorescence flow cytometry and biotinylation studies revealed a rapid increase in DAT cell-surface expression in response to D₂R stimulation. These experiments demonstrate that D_{2S}R stimulation increases DAT cell surface expression and therefore enhances substrate clearance. Furthermore, they show that the increase in DAT function is ERK 1/2-dependent but PI3K-independent. Our data also suggest the possibility of a direct physical interaction between DAT and D₂R. Together, these results suggest a novel mechanism by which D_{2S}R autoreceptors may regulate DAT in the CNS.

Dopamine (DA) is the predominant catecholamine neurotransmitter in the CNS. Dysregulation of DA neurons has been implicated in the pathogenesis of Parkinson's disease, schizophrenia and drug addiction (Sotnikova *et al.*, 2006). Extracellular DA levels are primarily regulated by the DA transporter (DAT), an integral membrane protein that is a member of the Na⁺/Cl⁻ dependent co-transporter gene family (Amara and Kuhar, 1993). By removing extracellular DA and recycling it back to the neuron, DAT plays an essential role in terminating DA signaling.

Receptor and second-messenger linked signal transduction pathways modulate DAT activity. Activation of protein kinase C (PKC) decreases transport capacity and promotes the redistribution of DAT from the plasma membrane to intracellular compartments (Loder and Melikian, 2003). More recently, modulation of DAT function and cell surface expression by extracellular signal-regulated kinases 1 and 2 (ERK 1/2) and phosphoinositide 3 kinase (PI3K) has been reported. Activation of ERK 1/2 increases transport capacity and similar effects are observed in response to PI3K activation (Carvelli *et al.*, 2002; Moron *et al.*, 2003).

In addition to their location postsynaptically or as heteroreceptors on the terminals of other neurons, dopamine 2 receptors (D₂R) are located on DA nerve terminals where their activation inhibits DA synthesis and release. They are also located on DA cell bodies where they function to inhibit cell firing. Studies in which voltammetric methods have been used to monitor the rate of DA clearance in the striatum have shown that D₂/D₃ receptor agonists increase the V_{max} of DA transport (Batchelor and Schenk, 1998; Meiergerd *et al.*, 1993), presumably through their action at presynaptic D₂Rs. Conversely, D₂R antagonists decrease DA clearance (Meiergerd *et al.*, 1993). This effect is absent in mice lacking the gene encoding D₂R (Dickinson *et al.*, 1999) suggesting a specific role of D₂R in regulating DAT function.

In *Xenopus laevis* oocytes heterologously expressing DAT and the long form of the D₂R (D_{2L}R), D_{2L}R-induced up-regulation of DA uptake occurs via a voltage-independent mechanism that is G_i/G_o dependent (Mayfield and Zahniser, 2001). However, D_{2L}Rs are primarily post-synaptic (Khan *et al.*, 1998), whereas the short form of D₂R (D_{2S}R) is located on DA terminals and serves an autoreceptor function. Therefore, fundamental questions remain as to the intracellular mechanisms by which D₂Rs regulate DAT. Indeed, increasing evidence suggests that the short and long D₂R isoforms may, at least in part,

differ in their downstream signaling pathways and may have different functions *in vivo* (Choi *et al.*, 1999; Usiello *et al.*, 2000).

D₂Rs signal via pertussis toxin-sensitive G proteins to a number of downstream effectors including adenylyl cyclase (Neve *et al.*, 2004; Choi *et al.*, 1999). Studies in striatal primary cultures and heterologous expression systems have shown that their stimulation also induces phosphorylation of ERK 1/2 (Brami-Cherrier *et al.*, 2002; Beom *et al.*, 2004). D_{2S}R-mediated phosphorylation of protein kinase B (Akt), a member of the serine/threonine kinase family and a major target of PI3K, has also been reported (Brami-Cherrier *et al.*, 2002; Burgering and Coffey, 1995), although a recent report has also demonstrated a novel arrestin-mediated mechanism for D₂R-induced inhibition of Akt (Beaulieu *et al.*, 2005). Recent work has shown that the PI3K pathway (Carvelli *et al.*, 2002) and the MAPK pathway (Moron *et al.*, 2003) modulate DAT function by altering cell surface expression, but their potential role in mediating the functional interaction of D_{2S}R with DAT is unknown.

Studies of DAT function typically assess [³H] DA uptake or clearance of exogenous DA. Importantly, however, DA binds with very high affinity to DA receptors (Sokoloff *et al.*, 1990). Therefore, its use in studies investigating D₂R regulation of DAT is not without confound since the concentration range of DA typically employed will result in D₂R activation. The present studies used the fluorescent DAT substrate, 4-[4-(diethylamino)-styryl]-N-methylpyridinium iodide (ASP⁺), which we show does not activate D_{2S}R, in combination with live cell imaging techniques (Schwartz *et al.*, 2003; Schwartz *et al.*, 2005; Mason *et al.*, 2005) to determine whether D_{2S}R activation upregulates DAT in heterologous expression systems and to identify the role of ERK 1/2 and PI3K signaling pathways in mediating this effect. Flow cytometry and biotinylation studies were conducted to determine whether upregulation is associated with an increase in DAT cell surface expression. BRET and co-immunoprecipitation techniques were used to explore whether D_{2S}R and DAT may be located in close proximity in cells co-expressing these two proteins.

METHODS

Materials- 2-(2-amino-3-methoxyphenyl)-4*H*-1-benzopyran-4-one (PD98059), 2-(4-morpholinyl)-8-phenyl-4*H*-1-benzopyran-4-one hydrochloride (LY294002), (S)-(+)-(4*aR*,10*bR*)-3,4,4*a*,10*b*-tetrahydro-4-propyl-

2*H,5H*-[1]benzopyrano-[4,3-*b*]-1,4-oxazin-9-ol hydrochloride (PD128907) and quinpirole hydrochloride were obtained from Tocris Cookson Inc. (Ellisville, MO). 4-[4-(dimethylamino)-styryl]-*N*-methylpyridinium iodide (ASP⁺), S (-)-eticlopride hydrochloride, sulpiride and pertussis toxin were obtained from Sigma-Aldrich (St. Louis, MO).

Cell Culture- Flp-in T-rex 293 cells (Invitrogen, Carlsbad, CA) stably expressing FLAG-tagged D_{2s}R were used for studies assessing the ability of DAT substrates to activate D_{2s}R. All other experiments were conducted in EM4 cells, human embryonic kidney 293 cells stably expressing a macrophage scavenger receptor to increase their adherence to tissue culture plastic (R.A. Horlick, Pharmacopeia, Cranberry, NJ) or in Neuro-2a cells (N2a, American Type Culture Collection, Manassas, VA). EM4 cells were maintained in DMEM/F12 medium (50:50; Cellgro Mediatech, Inc., Herndon, VA) supplemented with 10% FBS. N2a cells were maintained in MEM (Cellgro Mediatech, Inc., Herndon, VA) supplemented with 10% FBS. They were grown in a humidified atmosphere at 37°C and 5% CO₂. Twenty four h after plating, cells were transiently transfected using Lipofectamine 2000 (Invitrogen) according to the manufacturer's instructions. Experiments were performed 48 h after transfection when cells were 70-90% confluent.

Cell-based ELISA for pERK activation- A phosphospecific cell based ELISA (modified from Versteeg *et al.*, 2000) for phosphorylated ERK 1/2 (p-ERK) was used to determine activation of D_{2s}R by the DAT substrates: DA (1 pM - 10 µM), tyramine (1 pM - 100 µM) and ASP⁺ (1 pM - 100 µM). Cells (50,000 cells/cm²) were seeded in 96-well plates in DMEM media supplemented with 10% FBS and grown at 37°C and 5% CO₂ for 24 h. Tetracycline (0.1 µM) was added for an additional 16-20 h to induce D_{2s}R expression. Cells were serum starved in serum free media for 2 h prior to substrate addition (100 µl). After 3 min, media was aspirated and cells were immediately fixed by adding 150 µl of 4% formaldehyde PBS solution for 30 min. Cells were permeabilized by addition of 0.1% Triton X-100 PBS solution (3 x 10 min). After blocking with 10% BSA in Triton/PBS solution for 1 h, cells were washed with Triton/PBS solution. Primary p-ERK monoclonal antibody (Cell Signaling Technology) was diluted 1:400 in Triton/PBS solution containing 5% BSA and cells were incubated with primary antibody for 1 h at room temperature. After washing cells 3 times with PBS/Triton solution, and 1 h incubation with HRP-

conjugated goat anti-mouse 2° antibody (Santa Cruz Biotechnology, 1:1000 dilution) in PBS/Triton solution containing 5% BSA, cells were again washed with Triton/PBS solution. Pierce supersignal Elisa Pico substrate (100 µl) was added to each well for 2 min, and the luminescence signal was measured with a BMG PolarStar reader. The values from each experiment were normalized to the basal level for that experiment, and the means and SEM are shown for these determinations from three independent experiments, each performed in triplicate. The data were analyzed with Graph Pad Prism using a one-site sigmoidal dose response curve.

ASP⁺ Uptake- For ASP⁺ experiments, cells were seeded on day one at 1 x10⁵ cells/ 35 mm Delta T petri dish (Bioprotech, Butler, PA). Between 40-100 cells were used for each experiment unless otherwise stated. These cells were pooled from at least 3 separate transfections, with a minimum of 2 dishes analyzed per transfection. EM4 or N2a cells were transiently transfected with human D_{2S}R tagged with either an N-terminal FLAG epitope (FLAG-D_{2S}R) or an N-terminal myc epitope (myc-D_{2S}R) and/or yellow fluorescent protein tagged human DAT (YFP-hDAT). The addition of these tags does not alter transporter-mediated [³H]-DA uptake or D_{2S}R function (Khoshbouei *et al.*, 2003; Guo *et al.*, 2003). For the N-terminal truncation studies, FLAG-tagged wild type human DAT (WT FLAG-hDAT) (Saunders *et al.*, 2000) and a functional N-terminally truncated FLAG-tagged hDAT lacking the first 55 amino acids (ΔN₁₋₅₅ FLAG-hDAT, unpublished results, N.S., J.A.J.) were used. A human D_{2S}R with a yellow fluorescent protein at its C-terminus (YFP-D_{2S}R) was used in these studies in order to enable cell visualization.

Immediately before experiments, growth media was removed and cells were washed 2 times in Krebs-Ringer-HEPES (KRH, in mM: 130 NaCl, 1.3 KCl, 2.2 CaCl₂, 1.2 MgSO₄, 1.2 KH₂PO₄, 10 HEPES and 1.8 g/l glucose, pH 7.4) buffer. After washing, fresh KRH was added to the culture dish which was then mounted on an UltraVIEW LCI spinning-disc confocal microscope (Perkin Elmer, Wellesley, MA).

Time-resolved quantification of DAT function in single cells was achieved using the fluorescent, high affinity DAT substrate, ASP⁺. Use of this fluorescent analog in conjunction with a fluorescently tagged transporter allowed monitoring of DAT and norepinephrine transporter function in single cells (Schwartz *et al.*, 2003; Mason *et al.*, 2005; Schwartz *et al.*, 2005). A within-cell design was used to assess the effects of D_{2S}R stimulation on ASP⁺ uptake. The microscope was focused on the center of a

monolayer of cells and background auto-fluorescence was determined by collecting an image immediately prior to replacement of the KRH buffer with that containing ASP⁺ (10 μ M). The rate (slope of the linear accumulation function) of ASP⁺ uptake was then measured for 1 min immediately before drug addition. Vehicle or agonist (quinpirole: 0.1 - 10 μ M; PD12897: 10 μ M) was added and the slope of ASP⁺ accumulation was again determined over a 1 min period. Control studies showed that ASP⁺ uptake by DAT was linear over the first 10 min after ASP⁺ addition, was temperature-dependent and inhibited by the DAT substrates, amphetamine and cocaine (Kivell *et al.*, 2004; Zapata, *et al.*, 2006, submitted). Images were collected every 20 s for 10 min to enable capture of ASP⁺ fluorescence (excitation: 488 nm, emission: 607-652 nm). The influence of the D2/D3 receptor antagonist, eticlopride (0.1 μ M), the MEK inhibitor, PD98059 (10 μ M; Alessi *et al.*, 1995), and the PI3K inhibitor, LY294002 (10 μ M; Vlahos *et al.*, 1994), on quinpirole (10 μ M)-evoked ASP⁺ uptake was assessed by preincubating cells with vehicle or inhibitor for 15 min at 37°C. ASP⁺ was then added and intracellular accumulation was measured before and after addition of vehicle or agonist as described above. The concentrations of inhibitors used were those previously shown to be selective for the specific kinase examined (Alessi *et al.*, 1995; Vlahos *et al.*, 1994).

Image analysis- ASP⁺ fluorescence accumulation was determined from the average pixel intensity at each time point accumulated within the cell using the UltraView software package (Perkin Elmer, Wellesley, MA), the boundaries of which were determined from a reference picture at the initial time point of YFP fluorescence (indicating the presence of YFP-hDAT or YFP-D_{2S}R at the plasma membrane). Values are expressed as percent change in ASP⁺ accumulation rate after addition of drug. The resultant data were analyzed using a one-way ANOVA followed by the Student Newman-Keuls test (SNK) or using Student's t-test. Tests were performed using the GraphPad Prism, 4.0 statistical software package (Graph Pad Software, Inc., San Diego, CA). A value of $p \leq 0.05$ was considered statistically significant.

Immunoblotting- EM4 cells were transfected as described above with FLAG-D_{2S}R and YFP-hDAT and serum starved in serum free media for 16-18 h before the assay. On the day of the assay, cells were treated for 15 min at 37°C with the kinase inhibitor or vehicle prior to the addition of quinpirole (10 μ M) for

1 min at 37°C. A 1 min time point was selected based on the results of ASP⁺ experiments. Following incubation, media was aspirated and boiling Laemmli buffer (62.5 mM Tris, pH 6.8, 20% glycerol, 2% SDS, 5% β-mercaptoethanol, and 0.01% bromophenol blue) was added directly to the wells. Lysates were then collected and boiled for 10 min. Proteins were separated by SDS-PAGE (4-20% Duramide gradient gel, Cambrex, Walkersville, MD) and blotted onto polyvinylidene difluoride membranes. The membranes were then blocked for 1 h at room temperature in TBS-T containing 5% nonfat milk. Phosphorylated ERK 1/2 (p-ERK) was detected using a rabbit polyclonal antibody specific for ERK 1/2 phosphorylated at residues threonine 202 and tyrosine 204. Phosphorylated Akt was detected utilizing a rabbit polyclonal antibody which detects levels of Akt only when phosphorylated at serine 473 (p-Akt). To control for differences in protein loading, blots were stripped with 2% SDS, 100 mM β-mercaptoethanol (β-ME) in 62.5 mM Tris (pH 6.8) for 1 h at 50°C and reprobed with a polyclonal antibody that recognizes total ERK 1/2 or total Akt. All kinase antibodies were purchased from Cell Signaling Technology, Inc. (Beverly, MA). Blots were visualized using a horseradish peroxidase conjugated secondary antibody (Upstate, Lake Placid, NY) with enhanced chemiluminescence reagents.

For quantification, films were scanned at high resolution using an HP Scanjet 7400c (Hewlett-Packard, Palo Alto, CA) and band densities were quantified using MetaMorph software (Molecular Devices, Downingtown, PA). The relative amounts of phosphorylated kinases were normalized against those of the corresponding total kinase. Data were analyzed by one-way ANOVA followed by the Student Newman-Keuls test or using Student's t-test with GraphPad Prism, 4.0. The significance level for all analyses was $p \leq 0.05$.

[³H]Tyramine Uptake- Uptake studies with [³H] tyramine were performed as described (Hastrup *et al.*, 2001). Tyramine was used for these studies since it exhibits much lower potency at D_{2S}R than does DA (see Fig. 1). Hemiagglutinin (HA) epitope tagged hDAT (HA 2EL hDAT) was constructed from a synthetic gene encoding the human dopamine transporter mutated to include an HA epitope tag in the second extracellular loop (Sorkina *et al.*, 2006). This construct allowed FACs analysis to measure surface DAT (see below). EM4 cells were transiently transfected with FLAG-D_{2S}R and HA 2EL hDAT. One day after transfection the cells were split and plated in poly-D-lysine coated 96 well plates. Forty-eight h after

transfection, when the cells were confluent, they were washed twice with 200 μ l buffer (130 mM NaCl, 1.3mM KCl, 10 mM HEPES, 1.2 mM MgSO₄, 1.2 mM KH₂PO₄, 2.2 mM CaCl₂, 10mM glucose, pH 7.4). Cells were incubated with quinpirole (10 μ M), or sulpiride (10 μ M) + quinpirole (10 μ M) for 1 min prior to addition of 66 nM [³H] tyramine. Nonspecific uptake was determined in the presence of 2 mM tyramine and was similar to that detected in the presence of a DAT blocker. After 1 min incubation at room temperature, uptake was terminated by aspiration and washing twice with ice cold buffer. Cells were lysed with 50 μ l of 1% Triton X 100 for 15 min. Two hundred μ l optiphase supermix scintillation fluid was added and radioactivity was determined in a Wallac 1450 microbeta counter.

DAT Trafficking- Biotinylation and flow cytometry were used to determine whether D_{2S}R stimulation alters DAT cell surface expression. Cell surface biotinylation and immunoblot analyses were performed as described (Li *et al.*, 2004) to quantify the amount of plasma membrane DAT protein. EM4 cells (100,000 cells/well) were seeded into 12 well plates containing DMEM/F12 medium supplemented with 10% FBS and penicillin (100 units/ml) and streptomycin (100 μ g/ml) in an atmosphere of 5% CO₂ and 95% humidity atmosphere at 37°C. After 24 h, cells were transfected with different expression plasmids together with DAT and myc-D_{2S}R receptor cDNA plasmids (0.9 μ g D_{2S}R receptor and 0.3 μ g DAT) using LipofectamineTM 2000 transfection reagent according to manufacturer's protocols. In all wells, the total amount of plasmid DNA was adjusted with corresponding empty vector. Cells were treated with vehicle or quinpirole (10 μ M) for 1 min after 48 h of transfection. At the end of the treatment, cells were washed two times with ice-cold PBS/Ca-Mg (138 mM NaCl, 2.7 mM KCl, 1.5 mM KH₂PO₄, 9.6 mM Na₂HPO₄, 1 mM MgCl₂, 0.1 mM CaCl₂, pH 7.3) and incubated with EZ link NHS-Sulfo-SS-biotin (1mg/ml) in 1XPBS/Ca-Mg for 30 min at 4°C. The reaction was quenched by two washes with cold 100 mM glycine in PBS/Ca-Mg and further incubation with 100 mM glycine in PBS/Ca-Mg at 4°C for 20 min. Then the cells were lysed in 500 μ l of radioimmunoprecipitation assay (RIPA) buffer (10 mM Tris-HCl, pH 7.5, 150 mM NaCl, 1 mM EDTA, 0.1% SDS, 1% Triton X-100, and 0.1% Na-deoxycholic acid) containing protease inhibitors (1 μ M pepstatin A, 250 μ M phenylmethylsulfonyl fluoride, 1 μ g/ml leupeptin, and 1 μ g/ml aprotinin) for 1 hr at 4°C with constant shaking. Lysates were centrifuged at 25,000g for 30 min at 4°C, and clear supernatants were incubated with streptavidin beads (100 μ l beads/400 μ l cell lysates from one

well) for 1 hr at room temperature. Beads were washed three times with RIPA buffer, and bound proteins were eluted with 50 μ l of Laemmli buffer (62.5 mM Tris, pH 6.8, 20% glycerol, 2% SDS, 5% β -mercaptoethanol, and 0.01% bromophenol blue) for 30 min at 22°C. Aliquots from total cell lysates (50 μ l) and unbound fractions (100 μ l), and all (50 μ l) of avidin bound samples were analyzed by immunoblotting with DAT-specific antibody. To validate the surface localization of biotinylated DAT protein, blots were stripped and reprobed with calnexin antibody (Stressgen Biotechnologies, Victoria, BC, Canada). Band intensities were quantified using NIH ImageJ (v. 1.32j). Exposures were precalibrated to insure quantitation within the linear range of the film and multiple exposures were taken to validate linearity of quantitation. DAT densities from total, nonbiotinylated (representing the intracellular pool) and biotinylated (representing the surface pool) fractions were normalized using levels of calnexin in the total extract and values averaged across four experiments. The data were analyzed by ANOVA followed by SNK.

Flow cytometry was performed in cells transiently transfected with cDNA for HA 2EL hDAT and empty vector, or HA 2EL hDAT and FLAG-D₂₅R. Cells were washed with PBS and incubated in the presence or absence of quinpirole (10 μ M) for 2 min at 37°C. After fixing the cells with 2% PAF, surface expression of HA-2EL hDAT was quantified by FACs analysis using an anti-HA as described previously (Costagliola *et al.*, 1998). The fluorescence of 10,000 cells/tube was determined using a Guava Easy Cite cytofluorometer (Guava Technologies). Cells transfected with empty vector served as negative controls. The effect of quinpirole was compared to that of vehicle treatment for each experiment, and the mean \pm SEM are shown for these determinations from three independent experiments, each performed in triplicate. The Student's t-test was used for statistical analysis.

Co-immunoprecipitation- Co-immunoprecipitation experiments were conducted as previously described (Gomes *et al.*, 2003). EM4 cells were transiently transfected with cDNA for myc-D₂₅R, WT FLAG-hDAT or Δ N₁₋₅₅ FLAG-hDAT either alone or in combination (Guo *et al.*, 2003). Receptor-transporter complexes were solubilized in radioimmunoprecipitation buffer (10 mM Tris-HCl, pH 7.5, 150 mM NaCl, 1 mM EDTA, 0.1% SDS, 1% Triton X-100, and 0.1% Na deoxycholate) containing 10 mM iodoacetamide and protease inhibitor cocktail (Sigma-Aldrich) for 1 h at 4°C and centrifuged for 15 min in a microcentrifuge at 14,000

rpm. Lysates were immunoprecipitated with polyclonal anti-myc antibodies (rabbit, clone A-14, Santa Cruz Biotechnology, Santa Cruz, CA). The anti-myc antibodies were pulled down with Protein A-linked agarose beads, washed several times and eluted in Laemmli sample buffer. The immunoprecipitate was subjected to SDS-PAGE as described above and subsequently immunoblotted with monoclonal anti-FLAG antibodies (mouse, M2, Sigma-Aldrich, St. Louis, MO) to detect DAT. In other studies, FLAG-D₂₅R was transfected as above with and without YFP-hDAT. Complexes were immunoprecipitated with the M2 monoclonal anti-FLAG antibodies as described above and pulled down with Protein G-linked agarose beads. Proteins were visualized with a monoclonal DAT antibody (rat, MAB369, Chemicon, Temecula, CA). In addition, myc-D₂₅R was transfected as above with and without YFP-hDAT. Complexes were immunoprecipitated with polyclonal anti-myc antibodies, pulled down with Protein A-linked agarose beads and proteins were visualized with the monoclonal DAT antibody as described above.

BRET Assay- Human embryonic kidney cells (HEK-293) were transfected with either human D₂₅R with a luciferase on the C-terminus (2 µg; D₂₅R-Luc) alone or in combination with YFP-hDAT (2 µg) using Lipofectamine (Invitrogen, Carlsbad, CA) as per manufacturer's protocol. Cells were detached from plates 48 h after transfection by incubation with PBS containing 1 mM EDTA for 2 min, collected by centrifugation, washed with PBS and resuspended to ~1-2 x 10⁶ cells/ml with PBS containing 1 mM EDTA. Cells (2 ml) were placed in a cuvette, coelenterazine h was added to 5 µM final concentration and light emission was monitored from 420 to 590 nm at 5 nm intervals for 0.5 s using a FluoroMax-2 spectrometer (Jobin Yvon Spex Instruments, Edison, NJ). For BRET assays using the Fusion Microplate Reader, transfected cells (1x10⁵ cells/well) were plated in complete media onto a 96 well microplate (Optiplate-96, Perkin Elmer, Wellesley, MA). The next day, wells were washed 3 times with PBS, treated with 5 µM coelenterazine h and readings collected using a FusionTM Universal Microplate Reader (Perkin Elmer, Wellesley, MA). BRET ratios were calculated as described by Angers *et al.* (Angers *et al.*, 2000). As a positive control, a concurrent set of cells was transfected with luciferase-tagged κ opioid receptors (2 µg; κ-Luc) alone and in combination with YFP-tagged δ opioid receptors (2 µg; δ-YFP). Functional interactions between κ and δ opioid receptors have previously been reported and the receptors have been shown to be in close proximity (< 100 Å) using co-immunoprecipitation and BRET (Gomes *et al.*,

2002). In contrast to κ and δ opioid receptors, previous studies have shown no association of D_2R with the chemokine receptor, CCR5. Therefore, negative control studies were also conducted in cells co-transfected with human CCR5 tagged on the C-terminus with YFP (2 μ g; YFP-CCR5) and $D_{2S}R$ -Luc.

RESULTS

DA and Tyramine, but not ASP^+ , Activate $D_{2S}R$

Addition of DA to cells expressing $D_{2S}R$ resulted in a concentration-dependent increase in pERK1/2 (EC_{50} = 5 nM; Fig. 1). The DAT substrate tyramine showed a similar maximal effect but a much lower potency (EC_{50} = 1 μ M; Fig. 1). In contrast, no increase in pERK1/2 was seen with ASP^+ at concentrations as high as 100 μ M (Fig. 1).

Activation of $D_{2S}R$ Upregulates DAT Function

ASP^+ rapidly accumulated in the cytoplasm of EM4 cells co-expressing $D_{2S}R$ and DAT (Fig. 2 A, B). In contrast, little accumulation was observed in cells lacking DAT. Consistent with previous studies with NET (Schwartz *et al.*, 2003) two distinct phases of incorporation of the ASP^+ signal were observed. Binding of ASP^+ to transporters located on the cell surface was rapid (msec) and was followed by a second, slower (sec/min) phase of accumulation of ASP^+ signal in the cytoplasm (Fig. 2C). Addition of quinpirole to EM4 cells co-expressing FLAG- $D_{2S}R$ and YFP-hDAT increased the rate of ASP^+ accumulation (Fig. 2C, 3A). This effect was significant in response to 10 μ M quinpirole. Increased ASP^+ accumulation was also observed in response to PD128907, a structurally different D_2/D_3 receptor agonist (Fig. 3A). Cells were pretreated with vehicle or eticlopride, a D_2R antagonist, prior to the addition of quinpirole (10 μ M) to determine whether the increase in accumulation was $D_{2S}R$ -mediated. Eticlopride (100 nM) prevented the quinpirole-evoked increase in ASP^+ accumulation (ANOVA: $F_{(3,113)} = 12.4$; $p \leq 0.0001$; SNK: $p \leq 0.001$). ASP^+ accumulation in quinpirole-treated cells was increased by $31.4 \pm 6.7\%$ ($n=35$) from pre-drug levels as compared to $3.4 \pm 3\%$ in eticlopride + quinpirole treated ($n=41$) cells (data not shown). Incubation of cells with either vehicle ($2.7 \pm 4\%$; $n=25$) or eticlopride ($-0.8 \pm 2.6\%$; $n=30$), alone, did not alter ASP^+ accumulation. In EM4 cells transiently transfected with WT FLAG-hDAT and D_1 DA receptors (D_1R), addition of the selective D_1R agonist B135 (10 μ M) did not alter ASP^+ uptake; indicating that in contrast to $D_{2S}R$, D_1R activation is ineffective in modulating DAT activity (Zapata et al.,

2006, submitted). To determine whether D_{2S}R activation upregulates DAT function in a neuroblastoma cell line, ASP⁺ accumulation was quantified in N2a cells co-expressing FLAG-D_{2S}R and YFP-hDAT. Quinpirole (1 μM) induced a significant increase in ASP⁺ accumulation relative to vehicle-treated cells (Fig. 3B).

D_{2S}Rs are G protein-coupled receptors that signal primarily through the pertussis toxin-sensitive G_i/G_o class of heterotrimeric G proteins (Choi *et al.*, 1999). To test whether the interaction of D_{2S}R with DAT is G_i/G_o dependent, EM4 cells expressing FLAG-D_{2S}R and YFP-hDAT were incubated with pertussis toxin (100 ng/ml) for 16-24 h and the ability of quinpirole (10 μM) to increase ASP⁺ uptake was assessed. Pre-incubation with pertussis toxin prevented the quinpirole-evoked increase in ASP⁺ uptake (Fig. 4) suggesting that the D_{2S}R-mediated increase in DAT function requires coupling to G_i/G_o proteins. No difference between vehicle and pertussis toxin-treated cells in the rate of ASP⁺ accumulation prior to the addition of quinpirole was seen. The slopes normalized for DAT expression levels were 0.00072 ± 0.00005 and 0.00064 ± 0.00004, respectively, for vehicle and pertussis toxin-treated cells (data not shown).

Dopamine D_{2S}R modulates DAT function via an ERK 1/2-dependent, PI3 kinase-independent mechanism

D_{2S}Rs have been shown to signal via ERK 1/2 and PI3K in brain and various cell lines (Beom *et al.*, 2004; Bami-Cherrier *et al.*, 2002). Similar to our results in the intact cell ELISA with DA (Fig. 1), quinpirole (10 μM, 1 min, 37°C incubation) evoked a 2.8-fold increase in phosphorylated ERK 1/2 in EM4 cells co-expressing FLAG-D_{2S}R and YFP-hDAT as detected by immunoblotting (Fig. 5A). Preincubation with the MEK inhibitor, PD98059 (10 μM, 15 min, 37°C; Fig. 5A) prevented the quinpirole-evoked ERK 1/2 phosphorylation in these cells. In contrast, the PI3K inhibitor LY294002 (10 μM, 15 min, 37°C preincubation) was without effect (data not shown, Student's t-test, t=0.532, p=0.605 df=11).

Akt, a serine/threonine protein kinase, is a major target of PI3K via its pleckstrin homology domain (Burgering and Coffey, 1995). To determine whether D_{2S}Rs couple to PI3K in EM4 cells, phosphorylation of the Ser473 residue of Akt was assessed by immunoblotting (Fig. 5B). Quinpirole evoked a 2.5-fold increase in phosphorylated Akt in EM4 cells co-expressing FLAG-D_{2S}R and YFP-hDAT relative to that observed in vehicle treated cells co-expressing the two proteins. This increase was

blocked by preincubation with LY294002 (10 μ M, 15 min, 37°C; Fig. 5B) confirming its mediation by PI3K. In contrast, preincubation of cells with PD98059 (10 μ M, 15 min, 37°C) was without effect on Akt phosphorylation (data not shown, Student's t-test, $t=0.291$, $p=0.776$, $df=12$). These findings confirm that D_{2S}Rs activate ERK 1/2 as well as PI3K and show that D_{2S}R activation of ERK 1/2 occurs independently of PI3K in the EM4 cell line.

To determine the involvement of ERK 1/2 and PI3K in mediating DAT regulation by D_{2S}R, EM4 cells expressing FLAG-D_{2S}R and YFP-hDAT were incubated with either PD98059, LY294002 or vehicle for 15 min at 37°C prior to addition of quinpirole (10 μ M). ASP⁺ accumulation was measured before and after addition of quinpirole, as detailed in Methods. Preincubation with PD98059 (10 μ M, 15 min, 37°C) prevented the quinpirole-induced increase in DAT activity (Fig. 5C). In contrast, the PI3K inhibitor LY294002 (10 μ M, 15 min, 37°C preincubation) was without effect (Fig 5C). Concentrations of LY294002 as high as 30 μ M were also without effect (data not shown).

Influence of D_{2S}R activation on ASP⁺ accumulation in cells expressing N-terminally truncated DAT

The N-terminus of DAT contains a number of serine and threonine residues that are potential phosphorylation sites for ERK 1/2. To determine whether the first 55 amino acids of DAT are necessary for the functional interaction of D_{2S}R with DAT, EM4 cells were co-transfected with YFP-D_{2S}R and either WT FLAG-hDAT or Δ N₁₋₅₅ FLAG-hDAT. ASP⁺ accumulation was measured before and after addition of 10 μ M quinpirole. Quinpirole significantly increased the rate of ASP⁺ accumulation in cells expressing YFP-D_{2S}R and WT FLAG-hDAT (vehicle: 6.2 ± 2.5 ; $n=67$; quinpirole: 33.3 ± 2.8 ; $n=81$; $t=7.1$, $df=146$, $p \leq 0.0001$; data not shown). The magnitude of this effect did not differ from that observed in cells transfected with FLAG-D_{2S}R and YFP-hDAT (Fig. 2D). A similar D_{2S}R-mediated increase in ASP⁺ accumulation was observed in cells expressing Δ N₁₋₅₅ FLAG-hDAT (vehicle: 9.6 ± 1.6 ; $n=72$; quinpirole: 30.2 ± 3.8 ; $n=63$; $t=5.2$, $df=133$, $p \leq 0.0001$ vs vehicle group Δ N₁₋₅₅ FLAG-hDAT) indicating that D_{2S}R regulation of DAT does not require the first 55 amino acids of DAT.

D_{2S}R activation increases transport activity of DAT

To determine whether D_{2S}R regulation of DAT can be observed with radiolabeled substrate, the influence of quinpirole (10 μ M) on [³H] tyramine uptake was determined in EM4 cells transiently transfected with FLAG-D_{2S}R and HA 2EL hDAT. Incubation of cells with 10 μ M quinpirole significantly increased [³H] tyramine uptake relative to that of vehicle-treated cells (Fig. 6A). (ANOVA $F_{(3,16)} = 7.01$ $p=0.0031$ SNK: $p \leq 0.01$ vs. vehicle). Pretreatment with sulpiride prevented the quinpirole-evoked increase in [³H] tyramine uptake ($p < 0.05$ vs. quinpirole) (Fig. 6A). Quinpirole failed to alter [³H] tyramine uptake in cells expressing hDAT but not D_{2S}R (Fig. 6A), and sulpiride was also without significant effect on uptake in these cells (ANOVA $F_{(3,16)} = 0.05$ $p > 0.98$).

D_{2S}R activation regulates DAT cell surface expression

In view of the results obtained with ASP⁺ and [³H] tyramine, experiments were conducted to determine whether the D_{2S}R-mediated increase in DAT function was associated with altered surface expression of DAT. FACS analysis was used to detect DAT cell surface immunofluorescence in EM4 cells co-expressing FLAG- D_{2S}R and HA 2EL hDAT (Fig. 6B). Addition of 10 μ M quinpirole for 2 min significantly increased DAT cell surface immunofluorescence relative to vehicle treated cells (fold increase: 1.60 ± 0.24 ; $t=2.49$, $p < 0.05$, $df = 4$). In cells that were preincubated with sulpiride prior to addition of quinpirole, no alteration of cell surface fluorescence was seen (data not shown). In contrast, in cells expressing hDAT but not expressing D_{2S}R quinpirole was without significant effect (Fig. 6B) (fold increase: 1.06 ± 0.05 ; $t=1.11$, $p=0.2$, $df=4$).

Biotinylation studies, which permit quantification of cell surface and intracellular DAT, were conducted in EM4 cells co-expressing myc-D_{2S}R and FLAG-hDAT. Consistent with ASP⁺ uptake, tyramine uptake, and FACS analysis, incubation of cells for 1 min with quinpirole (10 μ M) significantly increased biotinylated DAT (surface) ($126 \pm 1.3\%$) and reduced non-biotinylated DAT (intracellular) ($65 \pm 4.2\%$; $F_{(1,7)} = 499$; $p \leq 0.0001$; SNK: $p \leq 0.0001$) indicating an increase in cell surface DAT (Fig. 7). Treatment with quinpirole did not alter the total amount of DAT protein as measured by immunoblotting. Less than 0.5% of total calnexin was present in streptavidin-bound fractions, indicating that cells were intact and intracellular proteins were not significantly biotinylated.

Co-immunoprecipitation and BRET studies to explore potential proximity of D_{2S}R and DAT

To determine whether DAT and D_{2S}R complexes could be isolated and to assess the involvement of the N-terminus of DAT in the potential interaction with D_{2S}R, solubilized lysates were prepared from EM4 cells co-expressing either myc-D_{2S}R and WT FLAG-hDAT or myc-D_{2S}R and NΔ₁₋₅₅ FLAG-hDAT or from a mixture of cells individually expressing myc-D_{2S}R and WT FLAG-hDAT or myc-D_{2S}R and NΔ₁₋₅₅ FLAG-hDAT and subjected to immunoprecipitation with an anti-myc antibody. When myc-D_{2S}R was co-expressed with either WT FLAG-hDAT or NΔ₁₋₅₅ FLAG-hDAT, immunoblotting with the anti-FLAG antibody revealed a ~100 kDa band corresponding to the molecular weight of hDAT (Fig. 8 lanes 2 and 4). This indicates that the N-terminus is not necessary for its participation in the immunocomplex with myc-D_{2S}R. No specific bands were observed with the FLAG antibody in the mixture of cells individually expressing the proteins (Fig. 8, lanes 1 and 3) or with untransfected EM4 cells (Fig. 8 lane 5), indicating that the presence of the myc-D_{2S}R/WT FLAG-hDAT or myc-D_{2S}R/NΔ₁₋₅₅ FLAG-hDAT complexes required expression in the same cell and was not simply an artifact of the solubilization and immunoprecipitation process. A faint 150 kDa band was observed in all lanes on the blots and corresponded to the rabbit anti-myc immunoprecipitation antibody (Fig. 8). The band was not present when the anti-myc immunoprecipitation antibody was omitted (data not shown). Diffuse larger molecular weight species were observed in blots from co-expressing cells, suggesting that a substantial fraction of the myc-D_{2S}R/WT FLAG-hDAT or myc-D_{2S}R/NΔ₁₋₅₅ FLAG-hDAT complexes were resistant to SDS/β-ME (Fig. 8, lanes 2 and 4). Under the same conditions described above, YFP-hDAT also co-immunoprecipitated with myc-D_{2S}R or FLAG-D_{2S}R selectively when co-expressed in cells, suggesting that the presence of different epitope tags does not interfere with the interaction (data not shown; see Methods for details).

The BRET assay was used to determine whether in living cells D_{2S}R and DAT might be in close enough proximity to interact (< 100 Å; Fig. 9). Cells co-expressing either luciferase-tagged D_{2S}R (D_{2S}R-Luc) and YFP-hDAT or D_{2S}R-Luc alone were treated with the luciferase substrate, coelenterazine h. Co-expression of D_{2S}R-Luc and YFP-hDAT resulted in a positive energy transfer signal, as evidenced by the increased BRET ratio (Fig 9, inset). The increased BRET ratio is comparable to that seen in experiments performed concurrently with cells co-expressing YFP-δ and κ-Luc opioid receptors (Fig. 9, inset) consistent with previous reports showing dimerization of these opioid receptor types (Gomes *et al.*, 2003;

Jordan and Devi, 1999). No energy transfer occurred when D_{2S}R-Luc was co-expressed with YFP-CCR5 (Fig. 9). These data suggest that upon transient co-transfection, some fraction of D_{2S}R and DAT appear to reside within 100 Å of each other (see below).

DISCUSSION

A live cell fluorescent imaging technique was used to show that D_{2S}Rs modulate DAT function and to identify the intracellular mechanisms mediating this effect. Our studies demonstrate that activation of D_{2S}R induces a rapid and pertussis toxin-sensitive increase in the rate of accumulation of the DAT substrate, ASP⁺, in mammalian cell lines co-expressing D_{2S}R and DAT. D_{2S}R activation induced phosphorylation of ERK 1/2 and Akt. Inhibition of ERK 1/2 prevented the D_{2S}R-mediated increase in ASP⁺ accumulation whereas inhibition of PI3K was without effect. FACS and biotinylation studies revealed increased DAT cell surface expression in response to D_{2S}R activation. Data obtained from co-immunoprecipitation and BRET studies show that some fraction of D_{2S}R and DAT appears to be in close proximity.

D₂Rs are enriched in striatum. Studies in which electrochemical techniques have been used to probe DAT function have provided evidence that D₂-like receptors regulate DAT in this brain region (Hersch *et al.*, 1997). Co-localization of D₂ receptors and DAT in axonal terminals has been reported providing an anatomical basis for the potential interaction of these proteins (Hersch *et al.*, 1997). However, two splice variants of the D₂ receptor, D_{2S}R and D_{2L}R, each with a distinct subcellular distribution, have been identified. D_{2S}Rs are enriched in presynaptic DA terminals, the site of DAT localization, whereas D_{2L}Rs are post-synaptic (Khan *et al.*, 1998). Although D_{2L}R modulation of DAT was reported in *Xenopus laevis* oocytes (Mayfield and Zahniser, 2001), whether D_{2S}Rs produce similar effects is unknown. *In vivo* and *ex vivo* studies seeking to address this issue are precluded by the absence of ligands that discriminate between them.

ASP⁺ is a fluorescent high affinity substrate of monoamine transporters (Schwartz *et al.*, 2003). De Felice and co-workers have shown that this substrate can be used with live cell immunofluorescence confocal microscopy to monitor norepinephrine transporter and DAT function in individual cells (Schwartz *et al.*, 2005; Mason *et al.*, 2005). ASP⁺ accumulates rapidly in HEK cells expressing DAT but not in non-

transfected cells. Accumulation is saturable and dependent upon pH and temperature. It is blocked by DAT inhibitors and substrates. These findings, which have been replicated in our laboratory, are consistent with those of radiometric and electrochemical studies and indicate that ASP⁺ accumulation reflects a transporter-mediated process.

The D₂/D₃ receptor agonist, quinpirole, induced an eticlopride-reversible increase in ASP⁺ uptake in EM4 cells co-expressing DAT and D_{2S}R. Increased uptake was observed in a response to a structurally distinct agonist, PD128907 and in N2a cells co-expressing D_{2S}R and DAT. In contrast, D₁ agonist treatment did not alter ASP⁺ accumulation in cells co-expressing DAT and D₁R. These data provide the first demonstration that D_{2S}R stimulation is sufficient to upregulate DAT function.

Pertussis toxin treatment prevented the quinpirole-evoked increase in ASP⁺ accumulation. Using *Xenopus laevis* oocytes, Mayfield and Zahniser (Mayfield and Zahniser, 2001) reported a pertussis toxin-dependent increase of DA uptake in response to D_{2L}R activation. Together, these data demonstrate that D₂Rs regulate DAT via a G_i/G_o-mediated process.

D₂ activation induces pertussin toxin-sensitive phosphorylation of ERK 1/2 and PI3K in striatum and heterologous cell systems (Brami-Cherrier *et al.*, 2002; Choi *et al.*, 1999 ; Kihara *et al.*, 2002). Since these kinase cascades regulate DAT function and cell surface expression (Carvelli *et al.*, 2002; Moron *et al.*, 2003), we examined whether D_{2S}R upregulates DAT via activation of these cascades. Immunoblotting revealed a rapid, quinpirole-evoked induction of pERK 1/2 in EM4 cells co-expressing D_{2S}R and DAT indicating that D_{2S}R activates ERK 1/2 in this cell line. Consistent with previous reports (Beom *et al.*, 2004), the MEK inhibitor, PD98059 prevented this effect. PD98059 pretreatment also prevented the increase in ASP⁺ accumulation produced by D_{2S}R activation. These data provide the first demonstration that D_{2S}R regulates DAT via an ERK 1/2-dependent mechanism. The PI3K inhibitor, LY294002, failed to modify the D_{2S}R increase in ASP⁺ accumulation indicating a specific role of the ERK 1/2 cascade in mediating the functional modulation of DAT by D_{2S}R. The lack of effect of LY294002 can not be attributed to the concentration employed since the same treatment regimen prevented D_{2S}R-mediated increases in Akt phosphorylation. Rather the differential effects of PI3K inhibition on Akt phosphorylation and ASP⁺ accumulation suggest a role of ERK 1/2, but not PI3K, in mediating D_{2S}R regulation of DAT. Interestingly, we have recently shown that D₃ DA receptors (D₃R) also upregulate DAT (Zapata *et al.*, 2006,

submitted). In contrast to D_{2S}R, both PI3K and ERK 1/2 inhibitors abolished the effect of D₃R activation on DAT function. Thus, although both D₂ and D₃ receptors regulate DAT function, they do so, at least in part, through different mechanisms.

The DAT N-terminus contains serine and threonine residues which are potential phosphoacceptor sites for PKC and ERK 1/2 (Lin *et al.*, 2003). N-terminal serines of DAT are phosphorylated in response to PKC activation (Foster *et al.*, 2002). Although this effect is not necessary for PKC-mediated DAT downregulation (Granás *et al.*, 2003), phosphorylation of these residues after treatment with DAT substrates (e.g., methamphetamine, amphetamine) is thought to be a mechanism by which psychostimulants promote transporter mediated DA efflux (Cervinski *et al.*, 2005). Data regarding the role of the DAT N-terminus or phosphoacceptor sites therein in the regulation of DAT function by other kinases or G-protein coupled receptors are limited (Granás *et al.*, 2003; Lin *et al.*, 2003). However, truncation of the 55 N-terminal residues of DAT did not alter D_{2S}R regulation of DAT, as quinpirole increased ASP⁺ accumulation similarly in cells expressing D_{2S}R and either WT FLAG-hDAT or Δ N₁₋₅₅ FLAG-hDAT. These data demonstrate that the DAT N-terminus is not necessary for modulation of DAT by D_{2S}R. Furthermore, they indicate that phosphorylation of serine or threonine residues contained therein does not mediate this effect.

Increased ASP⁺ uptake occurred within one minute after agonist addition suggesting mediation by a post-translational mechanism. Constitutive DAT trafficking between the plasma membrane and intracellular compartments has been reported (Loder and Melikian, 2003). Under basal conditions, DAT trafficks between the membrane and cytosol. Following its internalization, DAT is degraded or recycled back to the membrane. Cell surface biotinylation experiments that used an identical protocol to that in ASP⁺ experiments showed that brief D_{2S}R stimulation significantly increased cell surface DAT. This increase was accompanied by a significant decrease in intracellular DAT. Similarly, flow cytometry revealed increased DAT cell surface expression in cells expressing D_{2S}R and an epitope-tagged DAT. These data suggest that D_{2S}R activation increases DAT redistribution from the intracellular compartment to the cell surface, resulting in increased transport capacity. ERK1/2 activation increases cell surface DAT in heterologous expression systems (Moron *et al.*, 2003). Our results suggest that D_{2S}R increases DAT function and cell surface expression by activating this kinase cascade.

Co-immunoprecipitation studies suggest that, under some conditions, D_{2s}R and DAT may form a complex. When co-expressed, D_{2s}R can be immunoprecipitated with WT FLAG-hDAT or ΔN_{1-55} FLAG-hDAT. In contrast, no interaction occurred in a mixture of individually expressing cells. Of note, the DAT N-terminus was not necessary for co-immunoprecipitation, just it was not essential for D_{2s}R-mediated modulation of DAT function. Although caution is necessary in the interpretation of co-immunoprecipitation of membrane proteins from detergent lysates (Salim *et al.*, 2002), BRET revealed energy transfer between D_{2s}R fused to luciferase and DAT fused to yellow fluorescent protein, suggesting they are in close proximity. Importantly, however, at high expression levels and single acceptor/donor ratios substantial energy transfer can arise from random interactions within the membrane (James *et al.*, 2006). Furthermore, it is unclear whether the interaction takes place on the cell surface and/or in internal membranes.

Although BRET and co-immunoprecipitation studies indicate that a fraction of D_{2s}R and DAT may be associated under particular circumstances, D_{2s}R regulation of DAT requires coupling to G_i/G_o proteins and ERK 1/2 activation. Therefore, coupling to intracellular signaling pathways rather than a direct physical interaction between D_{2s}R and DAT most likely underlies D_{2s}R-evoked DAT upregulation. Furthermore, since receptor activation occurs at the plasma membrane, DAT that is recruited to the plasma membrane from intracellular vesicles/endosomes is unlikely to have been physically associated with activated receptors already at the plasma membrane. Additional studies are needed to determine whether an association of D_{2s}R and DAT occurs in native tissue and what, if any, role the potential proximity of these two proteins might play in regulating DAT.

We were able to confirm the D_{2s}R-mediated increase in transport using radiolabeled tyramine. However, the action of tyramine as a full agonist at D_{2s}R complicates its use in experiments in which the D_{2s}R is co-expressed, as some receptor activation will occur during the determination of uptake, particularly at high tyramine concentrations required for kinetic analysis. We show that use of DA as a substrate is not feasible given its potency at D_{2s}R. In contrast, ASP⁺ is inactive at the D_{2s}R and permits time-resolved quantification of transporter function in living cells. These data highlight the utility of the ASP⁺ imaging technique for exploration of the coupling between receptor activation and transport activity

In summary, the present studies describe activation of pERK 1/2 as a mechanism by which D_{2S}R autoreceptors modulates DAT cell surface expression, and consequently the effective concentration of extracellular DA in the synapse. Additional studies addressing the mechanisms relevant for this receptor-transporter interaction will be important for understanding the diverse mechanisms that regulate transporter activity.

Acknowledgments: This research was supported by the Intramural Research Program of the NIH, NIDA and NIH grants MH57324, MH54137 and DA11495 to J.A.J. and DA08863 and DA0019521 to L.A.D and NIDA and NIH grants P50DA015369 and MH062612 to S.R. We thank Dr. U. Gether for the gift of HA 2EL hDAT, Dr. F. Ciruela for the gift of the YFP-D_{2S}R cDNA, Dr. M. Bouvier for the gift of the YFP-CCR5 cDNA, Dr. O.W. Lindwasser for advice on FACS and Drs. L.J. DeFelice and J.W. Schwartz for their helpful advice on the ASP⁺ uptake technique.

REFERENCES

- Alessi DR, Cuenda A, Cohen P, Dudley D T and Saltiel A R (1995) PD 098059 Is a Specific Inhibitor of the Activation of Mitogen-Activated Protein Kinase Kinase in Vitro and in Vivo. *J Biol Chem* 270: 27489-27494.
- Amara SG and Kuhar M J (1993) Neurotransmitter transporters: recent progress. *Annu Rev Neurosci* 16: 73-93.
- Angers S, Salahpour A, Joly E, Hilairt S, Chelsky D, Dennis M and Bouvier M (2000) Detection of Beta 2-Adrenergic Receptor Dimerization in Living Cells Using Bioluminescence Resonance Energy Transfer (BRET). *Proc Natl Acad Sci U S A* 97: 3684-3689.
- Batchelor M and Schenk J O (1998) Protein Kinase A Activity May Kinetically Upregulate the Striatal Transporter for Dopamine. *J Neurosci* 18: 10304-10309.
- Beaulieu JM, Sotnikova T D, Marion S, Lefkowitz R J, Gainetdinov R R and Caron M G (2005) An Akt/Beta-Arrestin 2/2A Signaling Complex Mediates Dopaminergic Neurotransmission and Behavior. *Cell* 122: 261-273.
- Beom S, Cheong D, Torres G, Caron M G and Kim K M (2004) Comparative Studies of Molecular Mechanisms of Dopamine D2 and D3 Receptors for the Activation of Extracellular Signal-Regulated Kinase. *J Biol Chem* 279: 28304-28314.
- Brami-Cherrier K, Valjent E, Garcia M, Pages C, Hipskind R A and Caboche J (2002) Dopamine Induces a PI3-Kinase-Independent Activation of Akt in Striatal Neurons: a New Route to CAMP Response Element-Binding Protein Phosphorylation. *J Neurosci* 22: 8911-8921.
- Burgering BM and Coffer P J (1995) Protein Kinase B (c-Akt) in Phosphatidylinositol-3-OH Kinase Signal Transduction. *Nature* 376: 599-602.

Carvelli L, Moron J A, Kahlig K M, Ferrer J V, Sen N, Lechleiter J D, Leeb-Lundberg L M, Merrill G, Lafer E M, Ballou L M, Shippenberg T S, Javitch J A, Lin R Z and Galli A (2002) PI 3-Kinase Regulation of Dopamine Uptake. *J Neurochem* 81: 859-869.

Cervinski MA, Foster J D and Vaughan R A (2005) Psychoactive Substrates Stimulate Dopamine Transporter Phosphorylation and Down-Regulation by Cocaine-Sensitive and Protein Kinase C-Dependent Mechanisms. *J Biol Chem* 280: 40442-40449.

Choi EY, Jeong D, Won K, Park and Baik J H (1999) G Protein-Mediated Mitogen-Activated Protein Kinase Activation by Two Dopamine D2 Receptors. *Biochem Biophys Res Commun* 256: 33-40.

Costagliola S, Rodien P, Many M C Ludgate M, Vassart G (1998) Genetic Immunization Against the Human Thyrotropin Receptor Causes Thyroiditis and Allows Production of Monoclonal Antibodies Recognizing the Native Receptor. *J Immunol* 160: 1458-65.

Dickinson SD, Sabeti J, Larson G A, Giardina K, Rubinstein M, Kelly M A, Grandy D K, Low M J, Gerhardt G A and Zahniser N R (1999) Dopamine D2 Receptor-Deficient Mice Exhibit Decreased Dopamine Transporter Function but No Changes in Dopamine Release in Dorsal Striatum. *J Neurochem* 72: 148-156.

Foster JD, Pananusorn B and Vaughan R A (2002) Dopamine Transporters Are Phosphorylated on N-Terminal Serines in Rat Striatum. *J Biol Chem* 277: 25178-25186.

Gomes I, Filipovska J and Devi L A (2003) Opioid Receptor Oligomerization. Detection and Functional Characterization of Interacting Receptors. *Methods Mol Med* 84: 157-183.

Gomes I, Filipovska J, Jordan B A and Devi L A (2002) Oligomerization of Opioid Receptors. *Methods* 27: 358-365.

Granas C, Ferrer J, Loland C J, Javitch J A and Gether U (2003) N-Terminal Truncation of the Dopamine Transporter Abolishes Phorbol Ester- and Substance P Receptor-Stimulated Phosphorylation Without Impairing Transporter Internalization. *J Biol Chem* 278: 4990-5000.

Guo W, Shi L and Javitch J A (2003) The Fourth Transmembrane Segment Forms the Interface of the Dopamine D2 Receptor Homodimer. *J Biol Chem* 278: 4385-4388.

Hastrup H, Karlin A and Javitch J A. (2001) Symmetrical Dimer of the Human Dopamine Transporter Revealed by Cross-linking Cys-306 at the Extracellular End of the Sixth Transmembrane Segment. *Proc Natl Acad Sci U S A* 98: 10055-60.

Hersch SM, Yi H, Heilman C J, Edwards R H and Levey A I (1997) Subcellular Localization and Molecular Topology of the Dopamine Transporter in the Striatum and Substantia Nigra. *J Comp Neurol* 388: 211-227.

James JR, Oliveira MI, Carmo AM, Iaboni A, Davis SJ. (2006) A rigorous experimental framework for detecting protein oligomerization using bioluminescence resonance energy transfer. *Nat Methods*. 3:1001-6.

Jordan BA and Devi L A (1999) G-Protein-Coupled Receptor Heterodimerization Modulates Receptor Function. *Nature* 399: 697-700.

Khan ZU, Mrzljak L, Gutierrez A, De La C A and Goldman-Rakic P S (1998) Prominence of the Dopamine D2 Short Isoform in Dopaminergic Pathways. *Proc Natl Acad Sci U S A* 95: 7731-7736.

Khoshbouei H, Wang H, Lechleiter J D, Javitch J A and Galli A (2003) Amphetamine-Induced Dopamine Efflux. A Voltage-Sensitive and Intracellular Na⁺-Dependent Mechanism. *J Biol Chem* 278: 12070-12077.

Kihara T, Shimohama S, Sawada H, Honda K, Nakamizo T, Kanki R, Yamashita H and Akaike A (2002) Protective Effect of Dopamine D2 Agonists in Cortical Neurons via the Phosphatidylinositol 3 Kinase Cascade. *J Neurosci Res* 70: 274-282.

Kivell BM, Kahlig K, Galli A, Javitch J A, and Shippenberg T S (2004) Regulation of dopamine transporter function and cell surface expression by kappa opioid receptors. Washington, DC: *Society for Neuroscience Abstract Viewer/Itinerary Planner* 280.12.

Li LB, Chen N, Ramamoorthy S, Chi L, Cui XN, Wang L C, Reith M E (2004) The Role of N-glycosylation in Function and Surface Trafficking of the Human Dopamine Transporter. *J Biol Chem* 279: 21012-21020.

Lin Z, Zhang P W, Zhu X, Melgari J M, Huff R, Spieldoch R L and Uhl G R (2003) Phosphatidylinositol 3-Kinase, Protein Kinase C, and MEK1/2 Kinase Regulation of Dopamine Transporters (DAT) Require N-Terminal DAT Phosphoacceptor Sites. *J Biol Chem* 278: 20162-20170.

Loder MK and Melikian H E (2003) The Dopamine Transporter Constitutively Internalizes and Recycles in a Protein Kinase C-Regulated Manner in Stably Transfected PC12 Cell Lines. *J Biol Chem* 278: 22168-22174.

Mason JN, Farmer H, Tomlinson I D, Schwartz J W, Savchenko V, DeFelice L J, Rosenthal S J and Blakely R D (2005) Novel Fluorescence-Based Approaches for the Study of Biogenic Amine Transporter Localization, Activity, and Regulation. *J Neurosci Methods* 143: 3-25.

Mayfield RD and Zahniser N R (2001) Dopamine D2 Receptor Regulation of the Dopamine Transporter Expressed in *Xenopus Laevis* Oocytes Is Voltage-Independent. *Mol Pharmacol* 59: 113-121.

Meiergerd SM, Patterson T A and Schenk J O (1993) D2 Receptors May Modulate the Function of the Striatal Transporter for Dopamine: Kinetic Evidence From Studies in Vitro and in Vivo. *J Neurochem* 61: 764-767.

Moron JA, Zakharova I, Ferrer J V, Merrill G A, Hope B, Lafer E M, Lin Z C, Wang J B, Javitch J A, Galli A and Shippenberg T S (2003) Mitogen-Activated Protein Kinase Regulates Dopamine Transporter Surface Expression and Dopamine Transport Capacity. *J Neurosci* 23 : 8480-8488.

Neve KA, Seamans J K and Trantham-Davidson H (2004) Dopamine Receptor Signaling. *J Recept Signal Transduct Res* 24: 165-205.

Salim K, Fenton T, Bacha J, Urien-Rodriguez H, Bonnert T, Skynner HA, Watts E, Kerby J, Heald A, Beer M, et al. (2002) Oligomerization of G-protein-coupled receptors shown by selective co-immunoprecipitation. *J Biol Chem* 277: 15482-15485

Saunders C, Ferrer J V, Shi L, Chen J, Merrill G, Lamb M E, Leeb-Lundberg L M, Carvelli L, Javitch J A and Galli A (2000) Amphetamine-Induced Loss of Human Dopamine Transporter Activity: an Internalization-Dependent and Cocaine-Sensitive Mechanism. *Proc Natl Acad Sci U S A* 97: 6850-6855.

Schwartz JW, Blakely R D and DeFelice L J (2003) Binding and Transport in Norepinephrine Transporters. Real-Time, Spatially Resolved Analysis in Single Cells Using a Fluorescent Substrate. *J Biol Chem* 278: 9768-9777.

Schwartz JW, Novarino G, Piston D W and DeFelice L J (2005) Substrate Binding Stoichiometry and Kinetics of the Norepinephrine Transporter. *J Biol Chem* 280: 19177-19184.

Sokoloff P, Giros B, Martres M P, Bouthenet M L and Schwartz J C (1990) Molecular Cloning and Characterization of a Novel Dopamine Receptor (D3) as a Target for Neuroleptics. *Nature* 347: 146-51.

Sorkina T, Miranda M, Dionne K R, Hoover B R, Zahniser N R, Sorkin A. (2006) RNA Interference Screen Reveals An Essential Role of Nedd4-2 in Dopamine Transporter Ubiquitination and Endocytosis. *J Neurosci* 26: 8195-205.

Sotnikova TD, Beaulieu J M, Gainetdinov R R and Caron M G (2006) Molecular Biology, Pharmacology and Functional Role of the Plasma Membrane Dopamine Transporter. *CNS Neurol Disord Drug Targets* 5: 45-56.

Usiello A, Baik J H, Rouge-Pont F, Picetti R, Dierich A, LeMeur M, Piazza P V and Borrelli E (2000) Distinct Functions of the Two Isoforms of Dopamine D2 Receptors. *Nature* 408: 199-203.

Versteed HH, Nijhuis E, van den Brink G R, Evertzen M, Pynaert G N, van Deventer S J, Coofer P J, Peppelenbosch M P (2000) A New Phosphospecific Cell-Based ELISA for p42/p44 Mitogen-Activated Protein Kinase (MAPK), p38 MAPK, Protein Kinase B and cAMP-Response-Element-Binding Protein. *Biochem J* 350: 717-722.

Vlahos CJ, Matter W F, Hui K Y and Brown R F (1994) A Specific Inhibitor of Phosphatidylinositol 3-Kinase, 2-(4-Morpholinyl)-8-Phenyl-4H-1-Benzopyran-4-One (LY294002). *J Biol Chem* 269: 5241-5248.

FIGURE LEGENDS

Figure 1. Activation of D_{2S}R by DAT substrates. HEK 293 cells stably expressing FLAG-D_{2S}R were incubated with the indicated concentrations of the DAT substrates, DA, tyramine or ASP⁺ for 3 min at 37°C. Phosphorylation of ERK 1/2 (pERK 1/2) as determined in an intact cell ELISA was used to quantify D_{2S}R activation as described in "Materials and Methods." Data are expressed as the mean fold increase \pm S.E.M in pERK 1/2 from 3 experiments, each conducted in triplicate.

Figure 2. ASP⁺ Uptake in EM4 cells transiently co-transfected with myc- D_{2S}R and YFP-hDAT. (A) ASP⁺ rapidly accumulates in the intracellular compartment of EM4 cells co-expressing D_{2S}R and hDAT. (B) Accumulation is negligible in cells not expressing hDAT. (C) The time course of ASP⁺ uptake in a representative within cell experiment is shown. Note the initial rapid binding phase after ASP⁺ addition, followed by the linear uptake phase. Addition of quinpirole (10 μ M) increases the rate of ASP⁺ uptake relative to pre-drug values. The increase in DAT function is measured as a change in the slope of uptake measured within 1 min before and after addition of drug.

Figure 3. Activation of D_{2S}R upregulates DAT function. (A) EM4 cells were transiently co-transfected with FLAG-D_{2S}R and YFP-hDAT. DAT function was measured as accumulation of ASP⁺ fluorescence over time in cells treated with vehicle, quinpirole (0.1-10 μ M) or PD128907 (10 μ M). Data are expressed as the mean % increase \pm S.E.M. *** denotes significant difference of 10 μ M quinpirole from vehicle-treated cells (ANOVA: $F_{(3,182)}=8.45$ $p \leq 0.0001$; SNK: $p \leq 0.001$) and of 10 μ M PD128907 vs vehicle group (Student's t-test: $t=4.08$, $df=41$; $p \leq 0.001$). (B) N2a cells were transfected as above and quinpirole (0.1 μ M, 1 μ M)-evoked ASP⁺ accumulation was quantified. Data represent the mean % increase \pm S.E.M. ** denotes significant difference from vehicle-treated cells (ANOVA: $F_{(2,92)}=6.13$ $p \leq 0.01$; SNK: $p \leq 0.01$).

Figure 4. The D_{2S}R-mediated upregulation of DAT function is pertussis toxin-sensitive. EM4 cells transiently co-transfected with FLAG-D_{2S}R and YFP-hDAT were pre-treated 16-24 h with pertussis toxin (PTX, 100 ng/ml) and quinpirole (10 μ M)-evoked ASP⁺ accumulation was quantified. Data are expressed as mean % increase \pm S.E.M. (ANOVA $F_{(2,107)}=10.60$ $p \leq 0.0001$; SNK: *** $p \leq 0.001$).

Figure 5. The D_{2S}R-mediated upregulation of DAT function is ERK 1/2 sensitive and PI3K insensitive. (A) D_{2S}R signals via both ERK 1/2 and PI3K. Left panel: Immunoblot analysis of pERK 1/2 in EM4 cells transiently expressing FLAG-D_{2S}R and YFP-hDAT. Cells were pre-incubated for 15 min at 37°C with vehicle or PD98059 (10 μM) before stimulation with quinpirole (10 μM) for 1 min. Data are expressed as the mean ± S.E.M. fold increase in phosphorylated to total ERK 1/2 ratio from vehicle (ANOVA $F_{(3,27)}=23.84$ $p \leq 0.0001$; SNK: *** $p \leq 0.001$). Right panel: Immunoblot analysis of pAkt in EM4 cells pre-incubated for 15 min at 37°C with LY294002 (10 μM) before addition of quinpirole. Data represent the mean ± S.E.M. fold increase in phosphorylated to total Akt ratio from vehicle (ANOVA $F_{(3,31)}=25.33$ $p \leq 0.001$; SNK: *** $p \leq 0.001$). Representative immunoblots of at least three experiments are shown. (B) Inhibition of ERK 1/2 but not PI3K attenuates the quinpirole-evoked increase in ASP⁺ accumulation. EM4 cells were pre-incubated for 15 min with vehicle, PD98059 (10 μM) or LY294002 (10 μM) before addition of quinpirole (10 μM). ASP⁺ uptake was determined as described in Methods. ANOVA $F_{(3,108)}=12.23$ $p \leq 0.0001$; SNK: *** $p \leq 0.001$).

Figure 6. D_{2S}R stimulation increases tyramine uptake and DAT cell surface expression. EM4 cells were co-transfected with FLAG-D_{2S}R and HA 2EL hDAT (solid bars) or with HA 2EL and empty vector (open bars). (A) After 48 h cells were treated with or without quinpirole (10 μM) in the presence or absence of sulpiride (10 μM) for 1 min. ³H-tyramine uptake was determined as described in “Materials and Methods.” Data are expressed as the percent of vehicle treated uptake for the respective transfection conditions (mean ± SEM, n=5). Drug treatments were not significantly different from vehicle treatment for hDAT alone (ANOVA $F_{(3,16)} = 0.05$ $p>0.98$). In cells co-expressing D_{2S}R and hDAT, quinpirole induced a sulpiride-reversible increase in uptake (ANOVA $F_{(3,16)} = 7.01$ $p=0.003$ SNK: ** $p \leq 0.01$ vs. vehicle, [†] $p<0.05$ vs. quinpirole). (B) Cells were treated with or without quinpirole (10 μM) for 2 min and then were fixed and surface labeling was quantified with an anti-HA antibody and FACS analysis as described in “Materials and Methods.” Data are expressed as the percent of vehicle treated fluorescence for the

respective transfection conditions (mean \pm SEM, n=3). Quinpirole significantly increased fluorescence in cells co-expressing D_{2S}R and hDAT (t=2.49, df=4, * p<0.05).

Figure 7 D_{2S}R stimulation increases DAT cell surface expression

(A) EM4 cells were co-transfected with FLAG-hDAT and myc-D_{2S}R. After 48 hrs, cells were washed once with KRH buffer and incubated with biotinylating reagent with or without quinpirole (10 μ M) for 1 min. Isolation of biotinylated DAT and detection of DAT were performed as described under “Materials and Methods”. Western blots of DAT and calnexin from total lysates, avidin beads eluates and avidin beads unbound fractions are shown in the upper panel. Each blot is a representative of 4 separate experiments. Quantitative analysis of DAT band densities for 4 experiments (means \pm SEM) is shown in the lower panel. * indicates significant changes in biotinylated DAT compared to vehicle treatment (p < 0.05, one-way ANOVA with Bonferroni post-hoc analysis).

Figure 8. D_{2S}R co-immunoprecipitates both WT and N-terminally truncated DAT. Co-immunoprecipitation and immunoblot analysis of myc-D_{2S}R with WT FLAG-hDAT or Δ N₁₋₅₅ FLAG-hDAT. Lane 1: Lysates from EM4 cells individually expressing myc-D_{2S}R or WT FLAG-hDAT were mixed (mix) and immunoprecipitated (IP) with an anti-myc antibody and immunoblotted (IB) using an anti-FLAG antibody. Lane 2: Lysate from EM4 cells co-expressing (co) both proteins (myc-D_{2S}R and WT FLAG-hDAT) were subjected to the same procedure. Lane 3: Lysates from EM4 cells individually expressing myc-D_{2S}R or Δ N₁₋₅₅ FLAG-hDAT were mixed (mix) and treated as above. Lane 4: Lysate from EM4 cells co-expressing (co) both proteins (myc-D_{2S}R and Δ N₁₋₅₅ FLAG-hDAT) treated as above. Lane 5: Lysate from EM4 cells subjected to the same procedure as above. A representative blot of n=3 experiments is shown.

Figure 9. Energy transfer between D_{2S}R and DAT in live cells. HEK-293 cells were transiently co-transfected with the following pairs: D_{2S}R-Luc and YFP-hDAT; D_{2S}R-Luc and YFP-CCR5, κ -Luc and δ -YFP or transfected with D_{2S}R-Luc or κ -Luc alone and subjected to BRET analysis (see Methods). Light emission spectra of the different conditions are shown. Inset, BRET ratios as determined from data

obtained from the spectrophotometer or Fusion Microplate reader as described. Data are the mean \pm S.E.M., n=4.

Figure 1

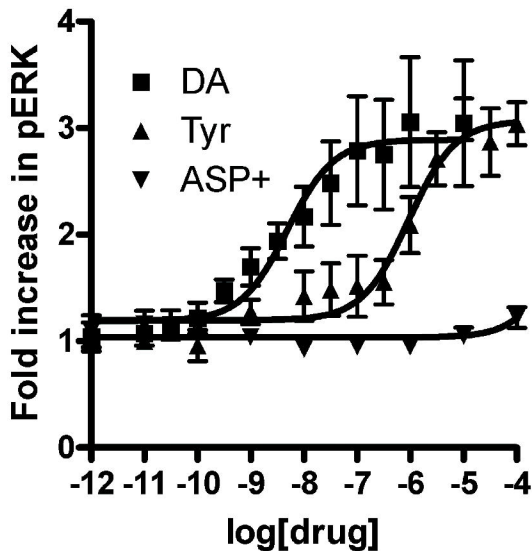


Figure 2

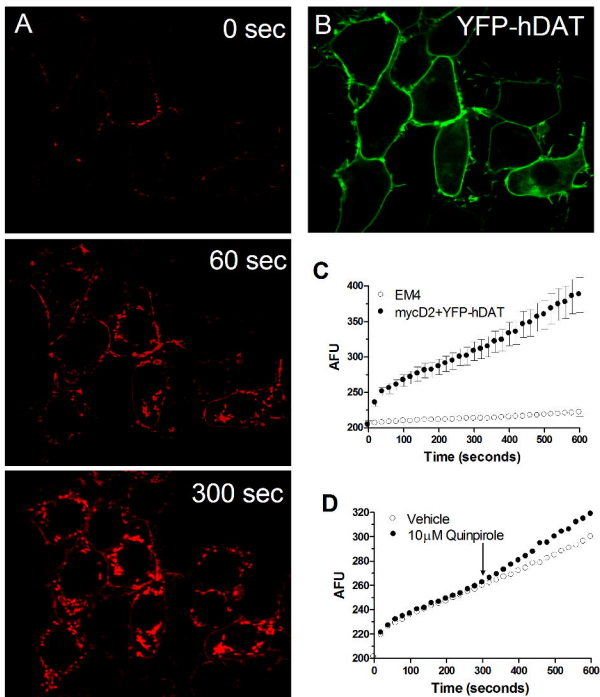


Figure 3

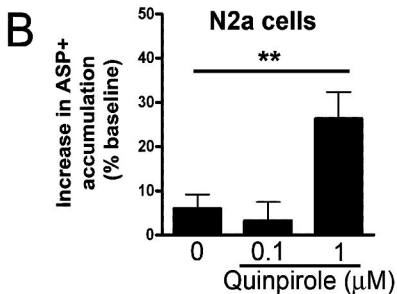
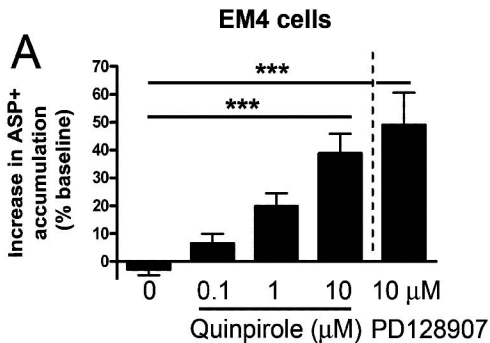


Figure 4

EM4 cells

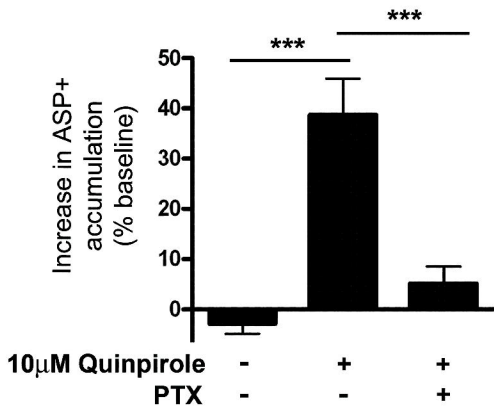


Figure 5

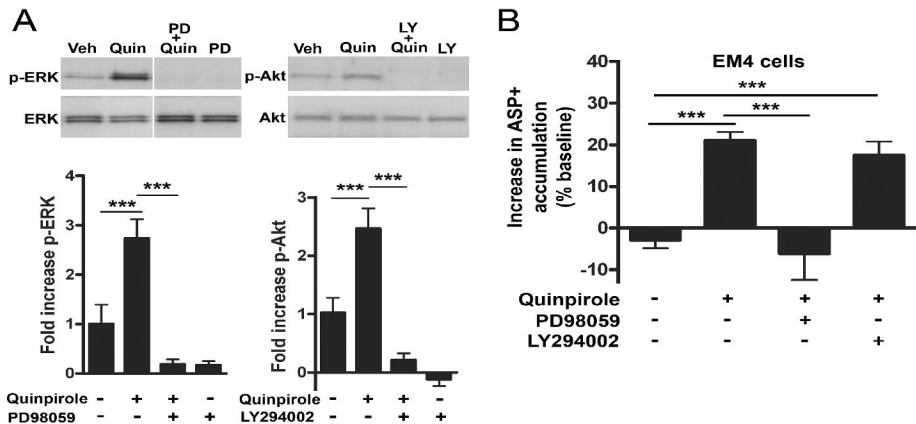


Figure 6

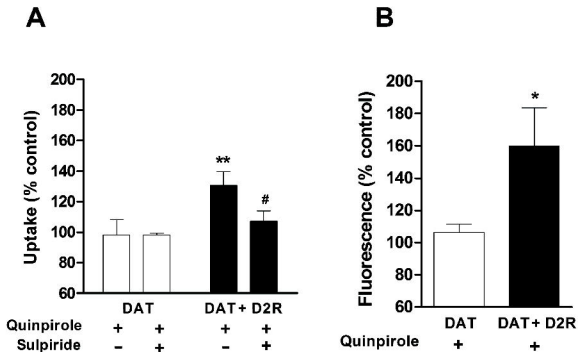
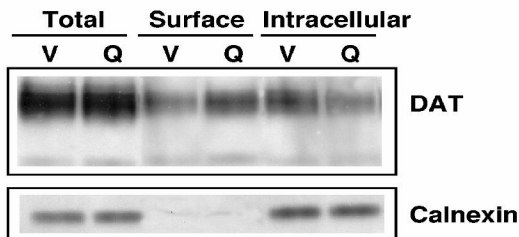


Figure 7

A



B

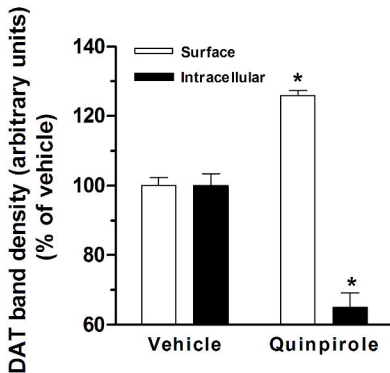


Figure 8

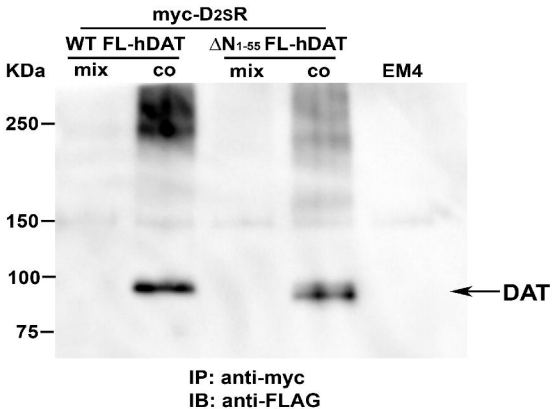


Figure 9

